Polymer Chemistry

Accepted Manuscript

ROYAL SOCIETY OF CHEMISTRY

www.rsc.org/polymers

Cite this: DOI: 10.1039/c0xx00000x

www.rsc.org/xxxxxx

PAPER

Synthesis and Biological Evaluation of Dual Functionalized Glutathione Sensitive Poly(Ester-Urethane) Multiblock Polymeric Nanoparticles for Cancer Targeted Drug Delivery

Arun Kumar,[a,b] Shantanu V. Lale,[a,b] Farhat Naz,[c] Veena Choudhary[d] and Veena Koul[a,b*]

Received (in XXX, XXX) Xth XXXXXXXXX 20XX, Accepted Xth XXXXXXXXX 20XX
DOI: 10.1039/b000000x

Glutathione sensitive polymeric nanoparticles comprising of poly(ester-urethane) and (-PCL-PEG-PCL-urethane-ss-) random multiblock copolymer with multiple disulfide linkages were developed for targeted doxorubicin delivery in cancer. The multiblock copolymers were synthesized via ring opening polymerization (ROP) of ε-caprolactone by polyethylene glycol followed by isomerization polymerization with hexamethylene diisocynate (HMDI) and 2-hydroxyethyl disulfide. Polyethylene glycol (PEG) content of ~20% in the multiblock copolymer led to formation of nanoparticles with size ~80 nm. High doxorubicin loading content of ~26% was achieved in the polymeric nanoparticles. Disulfide linkages in the multiblock copolymer facilitate nanoparticle degradation by glutathione (GSH) resulting in intracellular drug release. Drug release studies confirmed glutathione sensitive nature of polymeric nanosystem by achieving ~80% drug release at pH 5.5 in the presence of 10 mM GSH concentration as compared to ~19% at pH 7.4. *In vitro* studies in breast cancer cell lines (MCF-7 and BT474) showed ~20 fold increase in cellular uptake efficiency of dual targeted nanoparticles with subsequent higher apoptosis as compared to non-targeted polymeric nanoparticles. *In vivo* studies in Ehrlich's ascites tumor (EAT) bearing Swiss albino mice showed superior tumor regression of ~89% as compared to free doxorubicin (~42%) without any significant toxicity. The promising results show the potential of above synthesized multiblock copolymeric nanosystem as drug delivery nanocarrier in cancer therapeutics with enhanced antitumor efficacy and reduced toxicity.

1. Introduction

Doxorubicin, a potent anticancer drug, is an integral part of cancer chemotherapy, but it causes severe cardiotoxicity and also suffers from multidrug resistance. Various types of polymeric nanoparticles such as micelles, nanospheres, nanocapsules and polymersomes have been developed to overcome these limitations.[1-5] Polymeric nanosystems are easy to synthesize, scalable and can be functionalized with cancer specific ligands for active targeting. Amphiphilic block copolymers self-assemble to form micelles or polymersomes based on hydrophilic/hydrophobic ratio in the block copolymer.[6, 7] These nanosystems have been widely studied for passive and active targeting in cancer chemotherapy.[8-10]

Cancer cells exhibit redox rich environment with high cytoplasmic concentration of reducing agents such as glutathione (GSH). Glutathione, a tripeptide, is present in high concentration (1-10 mM) in cell cytoplasm while having very low concentration in blood plasma (2-20 μM).[11, 12] In tumor cells, the concentration of cytosolic GSH is several times higher than that in normal healthy cells.[13, 14] Thus, polymers with redox sensitive linkages would selectively release encapsulated drugs in cancer cells by trigger mechanism of high redox potential of cancer cells.[15, 16] Polymers containing redox sensitive disulfide linkages are widely used for drug delivery applications since they remain stable during circulation while release the drug after cellular uptake in cancer cells and thus hold promise for drug delivery in cancer chemotherapy.[17-20]

Active targeted drug delivery by ligand conjugation is widely used to increase selectivity and specificity of nanoparticles to cancer cells. In active targeting, ligands such as antibodies, aptamers, folic acid, sugars, hormones, peptides are often used.[21-23] Folic acid has been widely used for functionalization of polymeric nanoparticles since rapidly dividing cancer cells often over-express folate receptors to maintain increased requirement of folate in DNA synthesis.[9, 23] Human epidermal growth factor receptor (HER2) is often over-expressed in breast cancer and can be targeted by trastuzumab monoclonal antibody (Herceptin®).[24-26]

Polymer based on polyesters are widely used for drug delivery applications. Polyesters are widely synthesized via ring opening polymerization (ROP) of cyclic esters. Cyclic esters such as lactones are polymerized by ROP using organometallic compounds such as oxides and alkoxides (e.g. tin (II) octoate) as catalyst and alcohols as initiator to synthesize linear, star, brushes shaped polymers.[27, 28] Isomerization polymerization is widely used to synthesize multiblock copolymers with urethane linkages

using diisocyanate and diol monomers.[29-31]

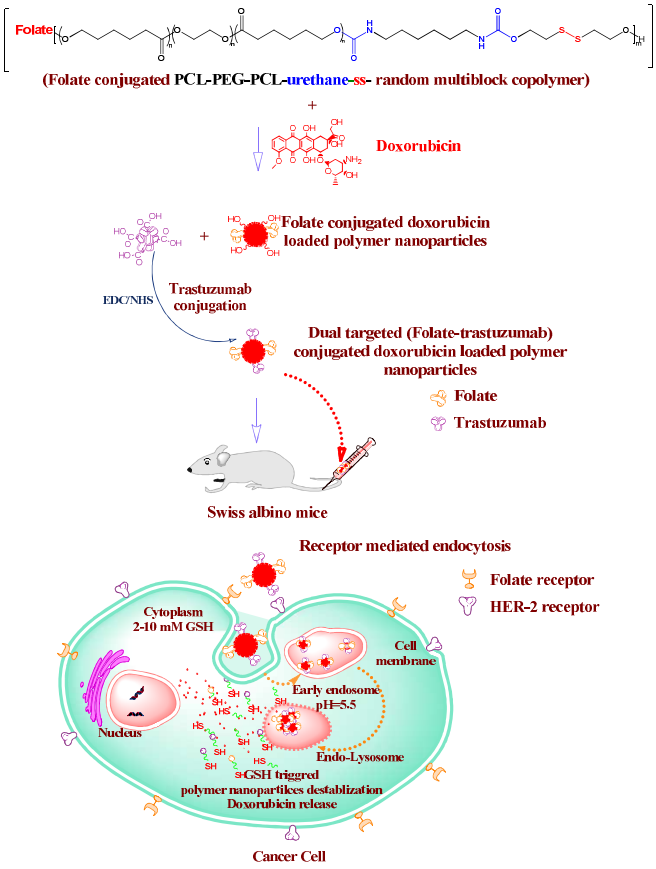

Scheme.1 Schematic representation of folate and trastuzumab conjugated glutathione sensitive multiblock polymeric nanoparticles for cancer targeting

Many polymeric nanocarriers based on multiblock copolymers with urethane and disulfide linkages have been reported for drug delivery applications in cancer.[32-35] Yu et al. developed pH and redox sensitive mPEG-polyurethane-mPEG polymer composed of methoxy polyethylene glycol (mPEG), bis(2-hydroxyethyl) disulfide, bis-1,4-(hydroxyethyl) piperazine and hexamethylene diisocyanate for intracellular cancer drug delivery.[36] Another paper published by Yu et al. also discusses disulfide cross-linked polymeric micelles based on PEG and polyurethane linkages bearing cyclic disulfide moieties (trans-4,5-dihydroxy-1-2-dithiane) and hexamethylene diisocyanate with end-capped mPEG for cancer therapeutics.[37] Li et al. reported redox responsive poly(ether urethane) composed of polyethylene glycol, N-methyl diethanolamine, hexamethylene diisocyanate and 2,2′-dithiodiethanol for preparing hydrogels for controlled protein drug delivery applications.[38]

Limitations of these nanosystems include non-biodegradability, absence of U.S. FDA approved polymers and lack of active targeting ability. So, it is need of the hour to develop actively targeted stimuli responsive polymeric nanocarriers prepared from biocompatible and biodegradable materials for drug delivery applications in cancer.

In this paper, we have developed and evaluated folic acid and trastuzumab functionalized redox sensitive polymeric nanoparticles based on poly(ester-urethane) and polycaprolactone -polyethylene glycol-polycaprolactone triblock copolymer (-PCL-PEG-PCL-urethane-ss-) random multiblock copolymer with multiple disulfide linkages in cancer (Scheme 1). A copolymer consisting of polyethylene glycol and polycaprolactone with multiple disulfide linkages was synthesized. Polyethylene glycol was introduced to increase circulation half-life of nanoparticles while polycaprolactone imparts biodegradability to the polymer. Multiple redox responsive disulfide linkages render selective drug release in cancer cells and also helps in biodegradation of the polymeric nanocarriers. The nanosystem was functionalized with folic acid and trastuzumab antibody for selective targeting of breast cancer cells. Together, polycaprolactone, polyethylene glycol, disulfide linkages and cancer targeting ligands impart multifunctional nature to the resulting nanosystem with biocompatibility, biodegradability, redox sensitivity, dual targetability and scalability.

After polymer synthesis, nanoparticle preparation and characterization, biocompatibility studies, drug loading and release studies of the nanosystem, *in vitro* and *in vivo* anticancer efficacy of the multifunctional nanosystem was carried out in breast cancer cell lines and in Ehrlich ascites tumor (EAT) bearing Swiss albino mice, respectively to evaluate the potential of the said nanosystem in combating the breast cancer.

2. Experimental

2.1. Materials

Poly(ethylene glycol) (PEG, M_n ~200 Da), ε-caprolactone, tin (II) 2-ethylhexanoate ($Sn(oct)_2$), 2-hydroxyethyl disulfide, hexamethylene diisocyanate (HMDI), dibutyltin dilaurate, (DBTL), N,N'-dicyclohexylcarbodiimide (DCC), 1-Ethyl-3-(3-dimethylaminopropyl)carbodiimide (EDC), N-hydroxysuccinimide (NHS), reduced glutathione (GSH), phosphotungstic acid (PTA) for staining, bovine serum albumin (BSA) and 3-(4,5-dimethyl-2-thiazolyl)-2,5-diphenyl-tetrazolium bromide (MTT) were purchased from Sigma-Aldrich (St. Louis, MO, USA) and used without further purification. Sodium bicarbonate ($NaHCO_3$), acetic acid, sodium acetate, and Triton X-100 were purchased from Merck Millipore (Mumbai, India) and used without further purification. Dialysis membrane of 3.5 kDa was obtained from Himedia (Mumbai, India). Herclon® (Trastuzumab for Injection) was purchased from Roche, India and used after purification by dialysis in PBS. Fetal bovine serum (FBS), penicillin-streptomycin solution and Dulbecco's modified Eagle's medium (DMEM) were purchased from Gibco Life Technologies (NY, USA). Doxorubicin was obtained as gift sample from Ranbaxy Laboratories Ltd, New Delhi, India. MCF-7, L929 and BT474 cells were obtained from NCCS, Pune India. Annexin V-FITC assay kit was obtained from BD Biosciences (San Jose, USA).

2.2. Synthesis of multiblock copolymers based on HO-PCL-PEG-PCL-OH

Synthesis of multiblock copolymers based on HO-PCL-PEG-PCL-OH triblock copolymer is a two-step reaction as shown in scheme 2. In the first step, HO-PCL-PEG-PCL-OH triblock copolymer was synthesized by tin octoate catalyzed ring opening polymerization of ϵ-caprolactone using PEG as initiator. In the

second step, various ratios of HO-PCL-PEG-PCL-OH triblock copolymer, 2-hydroxyethyl disulfide and hexamethylene diisocynate were taken for polymerization reaction to synthesize multiblock copolymers. Further, folic acid was conjugated to terminal hydroxyl group of multiblock copolymer via DCC-NHS coupling.

2.2.1. Synthesis of HO-PCL-PEG-PCL-OH triblock copolymer

Polyethylene glycol (M_n ~200 Da, 2 g, 10 mmol) was dissolved in toluene and azeotropic distillation was carried out to remove trace amounts of moisture. ϵ-caprolactone (3.5 equivalent, 3.87 g, 35 mmol) and tin-2-ethyl hexanaote (2 mol % of initiator, 81 µL) were added to the reaction medium in Schlenk tube and reaction was continued under N_2 atmosphere for 24 h at 110 °C. Toluene was evaporated on rotary evaporator after completion of the reaction and crude polymer was dissolved in dichloromethane and precipitated in cold diethyl ether. Product was dried and characterized by ^{1}H-NMR and gel permeation chromatography (GPC) (Perkin Elmer, USA). Yield= 90%.

^{1}H-NMR (300 MHz, $CDCl_3$, δ (ppm) - 1.34 (m,-$OCH_2CH_2\boldsymbol{CH_2}CH_2CH_2CO$-), 1.60 (m, $OCH_2\boldsymbol{CH_2}CH_2\boldsymbol{CH_2}CH_2CO$-), 2.29 (t, $OCH_2CH_2CH_2CH_2\boldsymbol{CH_2}CO$-), 3.63 (-$\mathbf{OCH_2CH_2}$-, PEG unit), 4.04 (t, -$O\boldsymbol{CH_2}CH_2CH_2CH_2CH_2CO$-), 4.24 (t, -$\boldsymbol{CH_2}$OH, terminal OH groups of PCL).

M_n (NMR) ~ 1408; M_n (GPC) = 1101 Da; M_w (GPC) = 1361 Da, molecular weight distribution = 1.24

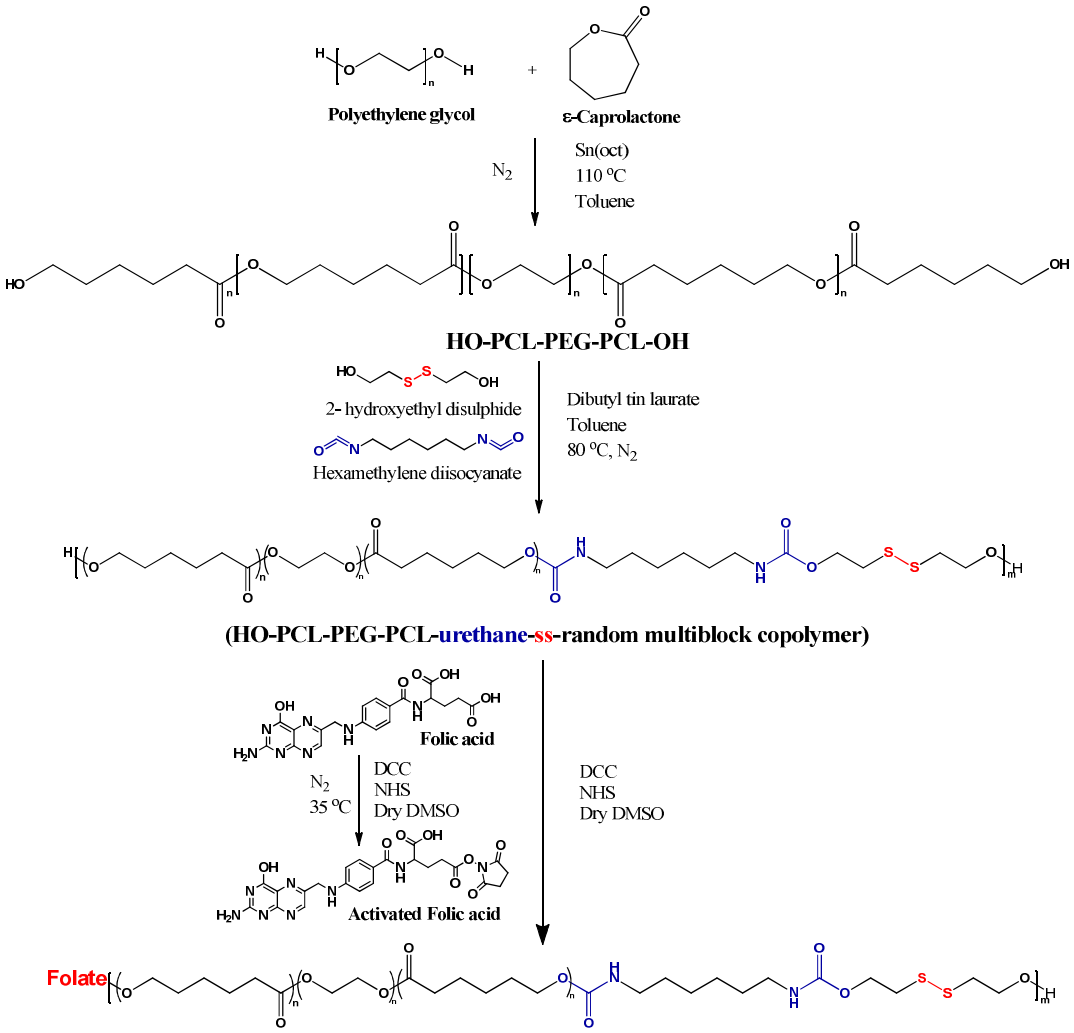

Scheme 2 Reaction scheme for folate conjugated random multiblock copolymer synthesis

2.2.2. Synthesis of the multiblock copolymer

Triblock copolymer HO-PCL-PEG-PCL-OH (2 g, 1.816 mmol), hexamethylene diisocyanate (341 µL, 2.12 mmol), 2-hydroxyethyl disulfide (30% of triblock copolymer, 67 µL, 0.545 mmol), toluene (10 mL) and dibutyl tin dilaurate (~59 µL, 0.1 mmol) were added to Schlenk tube and reaction was carried out for 12 h at 80 ºC under N_2 atmosphere. After completion of the reaction, toluene was removed and crude polymer was dissolved in dichloromethane and precipitated three times in diethyl ether. Product was isolated, dried and characterized by ^{1}H-NMR and GPC. Yield= 90%.

^{1}H-NMR (300 MHz, DMSO-d6, δ (ppm)) – 1.32 (m,-

$OCH_2CH_2\boldsymbol{CH_2}CH_2CH_2CO$- of PCL and -HN-$CH_2CH_2\mathbf{CH_2CH_2}CH_2CH_2$-NH- of hexamethylene group), 1.49 (m, $OCH_2\boldsymbol{CH_2}CH_2\boldsymbol{CH_2}CH_2CO$- of PCL), 2.07 (-HN-$CH_2\boldsymbol{CH_2}CH_2CH_2\boldsymbol{CH_2}CH_2$-NH- of hexamethylene group), 2.23 (t, $OCH_2CH_2CH_2CH_2\boldsymbol{CH_2}CO$- of PCL), 2.92 (m, -$CH_2\boldsymbol{CH_2}$ -SS-$\boldsymbol{CH_2}CH_2$- of 2-hydroxyethyl disulfide and -HN-$\boldsymbol{CH_2}CH_2CH_2CH_2CH_2\boldsymbol{CH_2}$-NH- of hexamethylene group), 3.49 (-OCH_2-CH_2-O of PEG unit), 3.95 (t, (-O-$\boldsymbol{CH_2}CH_2$ -SS-$CH_2\boldsymbol{CH_2}$-O-of 2-hydroxyethyl disulfide), 3.95 (t, $O\boldsymbol{CH_2}CH_2CH_2CH_2CH_2CO$- of PCL), 4.12 (t, -$\boldsymbol{CH_2}$OH terminal OH groups of PCL).

M_n (NMR) ~13000 Da. M_n (GPC) = 7789 Da; M_w (GPC) 13933 Da, molecular weight distribution = 1.78.

The reaction was also carried out by varying mole ratio of 2-hydroxyethyl disulfide (50% and 70% of triblock copolymer). The reaction details, yield and molecular weights are given in table 1.

Polymer Notation	HO-PCL-PEG-PCL-OH (mmol)	HMDI (mmol)	2-hydroxyl ethyl disulfide (mmol)	Yield (%)	$M_{n(GPC)}$	$M_{w(GPC)}$	PDI
MB-30-ss	1.816	2.125	0.545	90	7789	13933	1.78
MB-50-ss	1.816	2.452	0.908	88	9961	17074	1.71
MB-70-ss	1.816	2.787	1.27	94	29873	32505	1.08

Table 1. Polymer composition

2.2.3. Folic acid conjugation with the multiblock copolymer

Folic acid conjugation with the multiblock copolymer was carried out in two steps. In the first step, folic acid was activated by DCC-NHS. In a typical reaction, in Schlenk tube, Folic acid (81 mg, 0.184 mmol, 1.2 equivalent of copolymer) was dissolved in dry dimethyl sulfoxide (10 mL) followed by DCC (76 mg, 0.367 mmol) and NHS (42 mg, 0.367 mmol) and the reaction was stirred at 30 °C for 12 h under N_2 atmosphere. In the second step, the multiblock copolymer (MB-30-ss-) (2 g, 0.153 mmol) was added in Schlenk tube containing activated folic acid and allowed to stir at 30 °C for 12 h in presence of N_2. After the reaction, reaction mixture was dialyzed to remove unreacted folic acid and product was lyophilized. The yellow colored polymer thus obtained was characterized by energy dispersive X-ray spectroscopy (EDX, Bruker-AXS, QuanTax 200), FTIR (Perkin Elmer, USA) and by CHN analysis (Vario EL III Element Analyzer, Elementar Analysensysteme GmbH, Germany). Similarly, the reaction of folic acid to other multiblock copolymers MB-50-ss- and MB-70-ss- were also carried out.

2.3. Nanoparticle preparation and characterization

Nanoprecipitation method described by Fessi et al.[39] was used for nanoparticle preparation. Multiblock copolymer (10 mg) was dissolved in 1 mL dimethyl sulfoxide (DMSO) and added to 10 mL water with continuous stirring at 25 °C. Sample was then dialyzed with dialysis membrane (MWCO ~12K) for 4 h to remove DMSO followed by washing with Milli-Q water using Amicon ultracentrifuge filter (30 kDa) at 4000 rpm for 10 min at 25 °C. The obtained polymeric nanoparticles were lyophilized.

Polymeric nanoparticles were characterized using Zetasizer Nano ZS (DLS) (Malvern Instruments Ltd, UK) at 25 ºC. DLS were performed in triplicate with 0.1 mg/mL concentration of polymeric nanoparticle. The size and morphology of polymeric nanoparticles were analyzed by scanning electron microscopy (SEM, ZEISS EVO 50, Carl Zeiss Microscopy GmbH, Germany). The polymeric nanoparticle suspension (0.1 mg/mL) were deposited on a glass coverslip followed by air drying and coated with gold by ion sputtering (E1010, Hitachi, Japan). The morphology of polymeric nanoparticles was also observed by transmission electron microscopy (TEM, 200 kV Jeol 2100F field emission microscope, USA) by depositing stained samples of polymeric nanoparticles with 1% PTA on a carbon-coated copper grid. The surface morphological of polymeric nanoparticles was evaluated by atomic force microscopy (AFM) (Nanoscope III Digital Instrument 5.31R1, Digital Instruments, Inc. USA) by dispersing nanoparticles suspension on mica surface.

2.4. Colloidal stability of polymeric nanoparticles

Colloidal stability of polymeric nanoparticles (MB-30-ss) was studied in water, normal saline (0.9% w/v NaCl), 10 mM GSH and in DMEM media supplemented with 10% FBS using DLS for 24 h at 37 °C in the concentration of 0.1mg/mL.

2.5. Protein adsorption study

For protein adsorption studies, polymeric nanoparticles (5 mg) were incubated with 4% bovine serum albumin (BSA) solution (10 mL) in PBS at 37 ºC for 24 h in an incubator shaker at 100 rpm.The mixture was centrifuged at 26,200 rpm for 30 min, and the supernatant was quantified for protein content. Further biuret reagent (4 mL) was incubated with the supernatant (1 mL) at 37 °C for 30 min at 100 rpm. Unabsorbed protein was quantified by UV-vis spectrophotometer (BioTek PowerWave XS2) at 540 nm using calibration curve of known concentrations of BSA (500-2500 µg/mL).

2.6. Blood compatibility

Blood compatibility of polymeric nanoparticles was determined using hemolysis studies. Blood samples of healthy volunteer were obtained from blood bank facility, AIIMS, New Delhi, India. For hemolysis study of polymeric nanoparticles, RBCs were isolated from the blood by centrifugation at 1500 rpm for 5 min and further RBCs were washed with PBS. RBCs stock solution was prepared with 50 µL of RBCs in 10 mL PBS. Polymeric nanoparticles (100 µL) were incubated with 100 µL RBCs stock solution in concentration range 0.5-2 mg/mL at 37 °C for 30 min at 120 rpm in a shaker. The supernatant from the mixture was isolated by centrifugation at 1500 rpm for 5 min. UV-visible spectrophotometer was used to analyze the supernatant at 540 nm. The percentage hemolysis was quantified by using 1% Triton X 100 as positive control and PBS as negative control as per equation 1.

$$\% \text{ Hemolysis} = \frac{A_{Sample} - A_{Negative}}{A_{Positive} - A_{Negative}} \times 100 \quad (1)$$

Where, A_{Sample}, $A_{Negative}$ and $A_{Positive}$ are absorbance of nanoparticle, PBS and Triton X 100 treated samples respectively.

2.7. Drug loading and release

MB-30-ss polymer were used for drug loading on the basis of particle size. Doxorubicin loading was performed in the polymer nanoparticles according to Sanson et al.[40] Doxorubicin

hydrochloride (25 mg) and folate conjugated MB-30-ss polymer (50 mg) were dissolved in DMSO (5 mL). The DMSO solution was further added to 50 mL (50 mM) of carbonate buffer (pH 10.5) with continuous stirring. Excess doxorubicin and DMSO was removed by dialysis against Tris buffer (10 mM Tris, pH 7.4) for 6 h (MWCO 12-14 kDa). External Tris buffer was changed three times during dialysis. Drug loading content and encapsulation efficiency were calculated at 481 nm using UV-visible spectrophotometer (Perkin-Elmer Lambda 25, USA). Quantification of doxorubicin was performed on the basis of calibration curve of doxorubicin and by equation 2 and 3.

Drug loading content (%)

$$= \frac{Weight\ of\ drug\ loaded\ in\ nanoparticles}{Weight\ of\ nanoparticles} \times 100 \quad (2)$$

Drug encapsulation efficiency (%)

$$= \frac{Amount\ of\ Drug\ loaded\ in\ nanoparticles}{Total\ drug\ taken} \times 100 \quad (3)$$

For drug release studies, dialysis membrane (MWCO 12-14 kDa) containing 10 mL of drug loaded nanoparticles (0.8 mg/mL polymer concentration) were suspended in release media at 37 °C in incubator shaker (100 rpm) up to 96 h. Release media included PBS (pH 7.4) and acetate buffer (pH 5.5) with and without 10 mM GSH. Release studies were carried out in triplicate and at definite time intervals, aliquots (1 mL) were taken from the external medium and replaced with an equal volume to maintain sink condition.

2.8. Preparation of trastuzumab conjugated polymer nanoparticles

Polymer nanoparticles were conjugated to trastuzumab via EDC-NHS chemistry. Folate conjugated polymeric nanoparticles (MB-30-ss-FA-Dox NPs) were suspended in Milli-Q water (1 mg/mL) followed by addition of EDC (100 µL, 200 mmol), NHS (100 µL, 100 mmol). Trastuzumab (200 µL, 3 mg/mL in PBS) was added to the reaction medium and the reaction was allowed at 4 °C for 30 min. After the reaction, the polymer nanoparticles were washed with Milli-Q water using Amicon ultracentrifuge filter followed by lyophilization. Similarly, trastuzumab conjugated polymer nanoparticles (MB-30-ss-Her-Dox-NPs) were prepared from native non-conjugated polymer nanoparticles (MB-30-ss-Dox-NPs). Trastuzumab conjugated NPs were characterized by EDX, X-ray photoelectron spectroscopy (XPS) and zeta potential. Concentration of trastuzumab conjugated on the nanoparticle surface was further determined using Biuret assay. Unconjugated trastuzumab was quantified from the filtrate and was then subtracted from the initial trastuzumab concentration to obtain trastuzumab concentration conjugated with the nanoparticles. Composition of polymer nanoparticles with different type of attached ligands are shown in Table 2.

Table 2. Polymer nanoparticles compositions (MB-30-ss-NPs) depending on attached targeting moieties

Polymer nanoparticles notations	Composition
MB-30-ss-NPs	Native non-conjugated polymer nanoparticles
MB-30-ss-Dox-NPs	Native non-conjugated doxorubicin loaded polymer nanoparticles
MB-30-ss-FA-Dox- NPs	Folate conjugated doxorubicin loaded polymer nanoparticles
MB-30-ss-Her-Dox-NPs	Trastuzumab conjugated doxorubicin loaded polymer nanoparticles
MB-30-ss-FA-Her-Dox-NPs	Folate and trastuzumab conjugated doxorubicin loaded polymer nanoparticles

2.9. Cell line studies

2.9.1. MTT cell viability assay

Biocompatibility of polymeric nanoparticles was evaluated in BT474, MCF-7 (cancer cell lines) and L929 (normal murine cell lines) cells using MTT assay.[41] Cells at a density of 1×10^4 were added in 96 well with DMEM medium supplemented with 10% FBS and 1% penicillin-streptomycin and incubated for 24 h in CO_2 incubator at 37 °C. Polymeric nanoparticles in concentration range 0.25-2.0 mg/mL were incubated with cells for 24 h. PBS and 1% Triton X 100 were used as negative and positive control respectively. After 24 h, 10 µL MTT (5 mg/mL) were added to the wells and incubated for 4 h. The formazan crystals were formed which were dissolved in 200 µL dimethyl sulfoxide and absorbance was measured at 540 nm. Cell viability was calculated using equation 4.

$$\text{Cell viability } \% = \frac{A_{Sample} - A_{Positive}}{A_{Negative} - A_{Positive}} \times 100 \quad (4)$$

Where A_{sample}, $A_{negative}$ and $A_{positive}$ are the absorbance of cells treated with polymeric nanoparticles, PBS and 1% Triton X 100 respectively.

2.9.2. *In vitro* cellular uptake studies using confocal laser scanning microscopy

Cellular uptake analysis of non-conjugated and conjugated polymeric nanoparticles were carried out in BT474, MCF-7 and L929 cells. Cells at a density of 50,000 cells/well were added in six well plate and incubated in CO_2 incubator at 37 °C for 24 h. Polymer nanoparticles (doxorubicin concentration 10 µg/mL) were incubated with cells for 4h at 37°C in CO_2 incubator. After 4 h, cells were washed with PBS and were fixed with 4% paraformaldehyde buffer solution. Cells were stained with nuclear stain DAPI (20 µL) and were observed under CLSM at 100x magnification (Olympus Fluoview FV 1000, USA).

2.9.3. Cellular uptake studies using flow cytometry

Quantitative analysis of cellular uptake of polymeric nanoparticles was carried out in BT474, MCF-7 and L929 cells. Cells were seeded at a density of 1×10^5 cells in six well plates and incubated for 24 h in CO_2 incubator at 37 °C. Cells were then treated with polymer nanoparticles (doxorubicin concentration 10 µg/mL) and incubated in CO_2 incubator for 4 h at 37 °C. After 4 h cells were washed with PBS, trypsinized and centrifuged at 3500 rpm for 5 minutes and further washed with PBS. Cells were then suspended in 0.5 mL PBS for cellular uptake analysis by

flow cytometry (BD FACS Aria, BD Biosciences USA).

2.9.4. Apoptosis assay

Cellular apoptosis and necrosis studies were carried out in BT474, MCF-7 and L929 cell line using Annexin V-FITC kit. Cells at a density of 1×10^5 were seeded in six well plates and incubated in CO_2 incubator at 37 °C for 24 h. Polymer nanoparticles (doxorubicin concentration 10 µg/mL) were incubated with cells for 7 h. Cells were then washed three times with PBS, trypsinized and centrifuged at 3500 rpm for 5 minutes and further washed with PBS. Cells were then suspended in 0.5 mL Annexin binding buffer. Cells were incubated with 5 µL of Annexin V-FITC and 5 µL of propidium iodide solution in the dark for 20 min at 37 °C. The fluorescence of the cells was measured by flow cytometry and apoptotic/necrosis was determined based on differential staining- early apoptosis cells (positive with Annexin V-FITC and negative with propidium iodide), necrotic cells (positive with both Annexin V-FITC and propidium iodide) and live cells (negative with Annexin V-FITC and propidium iodide).

2.10. Animal studies

Animal studies were performed on Swiss albino mice (age 55-65 days, weight 25 ± 5 g). Mice were procured from central animal facility, All India Institute of Medical Sciences (AIIMS), New Delhi, India (Ethical approval number -796/IAEC/14). Ehrlich ascites tumor (EAT) cell line was procured from Dr B. S. Dwarakanath's lab, Institute of Nuclear Medicine and Allied Sciences (INMAS), New Delhi. All the animal experiments were carried out as per the guidelines of Committee for the Purpose of Control and Supervision on Experiments on Animals (CPCSEA). Throughout the whole study, the animals were maintained in environmentally controlled room and were fed chow food and purified water *ad libitum*. Animals were randomized into three groups consisting of six mice per group for the study. Group 1 free doxorubicin (5 mg/kg), group 2 MB-30-ss-FA-Her-Dox-NPs (doxorubicin concentration equivalent to 5 mg/kg) and group 3 PBS as control.

2.10.1. Tumor induction and regression studies

Ehrlich's ascites tumor (EAT) cells (2×10^7 cells) were subcutaneously injected in mice on the dorsal side for tumor induction and kept under observation for tumor onset. When the tumor volume reached ~200-250 mm^3, that day was designated as day zero and treatment (free doxorubicin and MB-30-ss-FA-Her-Dox-NPs equivalent to 5 mg/kg doxorubicin) was started via tail vein injections for 15 days with time interval of 3 days. Vernier caliper was used to measure tumor volumes and tumor volume was calculated using equation 5.

$$V = 0.5 \times L \times W^2 \quad (5)$$

Where V represents Volume, L represents length and W represents width of tumor in mm. Mice were sacrificed on 18^{th} day and blood was collected for serum biochemistry analysis.

2.10.2. Histopathological studies

To determine doxorubicin toxicity in vital organs of mice, all the animals were sacrificed on 18^{th} day and their heart, lungs, liver, kidneys, spleen along with tumor were removed and stored in 4% formalin buffer solution for histological analysis. The slides were prepared by cutting paraffin embedded organs into 5 µm thin sections using a rotary microtome (Leica, USA). Sections were stained with hematoxyline and eosin (H&E) and were studied under light microscope.

2.10.3. Serum biochemistry analysis

Blood samples from EAT bearing mice were obtained to analyze serum biochemical parameters. Serum samples were analyzed for various blood parameters like creatinine kinase (CK-MB) aspartate transaminase, alanine transaminase, alkaline phosphatase, cholesterol, creatinine, uric acid, total protein, albumin and globulin.

2.11. Statistics

All the data are expressed as mean ± standard deviation (SD). One way analysis of variance (ANOVA) was used using Sigma Stat (V.3.5 Systat Software Inc., San Jose, USA) with Bonferroni multiple comparison test. Statistical significance was considered at p value < 0.05.

3. Results and discussion

3.1. Synthesis and characterization of multiblock copolymer

The synthesis of folate conjugated multiblock copolymer based on HO-PCL-PEG-PCL-OH triblock copolymer is shown in scheme 2. First, triblock copolymer HO-PCL-PEG-PCL-OH was synthesized by ring opening polymerization of ϵ-caprolactone in presence of tin octoate as a catalyst. The ^{1}H-NMR confirmed successful synthesis of HO-PCL-PEG-PCL-OH triblock copolymer (Supporting Information Figure S1) According to ^{1}H-NMR spectrum, presence of characteristic peaks at δ 1.34, 1.60, 2.29 and 4.08 corresponding to polycaprolactone methylene units confirmed the synthesis of triblock polymer. Multiplet broad peak at δ 3.63 due to methylene units of PEG confirmed PEG units in the triblock copolymer. Molecular weight of triblock copolymer was calculated by ^{1}H-NMR and GPC. ^{1}H-NMR showed molecular weight of polymer to be ~1408 Da whereas GPC (Supporting Information Figure S2A) showed M_n and M_w of 1100 Da and 1395 Da respectively with molecular weight distribution of 1.26.

In the next step, multiblock copolymer were synthesized by varying molar ratios of 2-hydroxy ethyl disulfide. These components were taken in different ratio and polymerization was carried out in presence on dibutyl tin dilaurate at 80 °C. The multiblock copolymer was characterized by ^{1}H- NMR, FTIR and GPC. ^{1}H-NMR confirmed synthesis of the multiblock copolymer (Supporting Information Figure S3A). Multiplet peaks at δ 1.32 and δ 2.07 corresponds to methylene units of hexamethylene diisocyanate in the multiblock copolymer backbone due to the formation of urethane linkage. Triplet peak at δ 2.92 of methylene groups attached to disulfide group in 2-hydroxyethyl disulfide (-CH_2***CH_2***-SS-***CH_2***CH_2-) and triplet peak at δ 3.95 due to methylene group of 2-hydroxyethyl disulfide (-O-***CH_2***CH_2-SS-CH_2***CH_2***-O- confirmed incorporation of disulfide linkage in polymeric backbone. All the peaks corresponding to polycaprolactone and polyethylene glycol were retained in the ^{1}H-NMR spectrum. On the basis of ^{1}H-NMR integration, it was found that multiblock copolymer has ~3 units of 2-hydroxyethyl disulfide in the multiblock copolymer and thus three disulfide

linkages in one polymer chain.

Further, FTIR spectra of multiblock copolymer (Supporting Information Figure S4 A) was confirmed by N-H stretching vibration band at 3300 cm^{-1}. -NH-CO- stretching vibration band at 1682 cm^{-1} confirmed formation of urethane linkages in the multiblock copolymer. Vibration band at 1722 cm^{-1} confirmed presence of ester linkage in the polymer. The molecular weight of multiblock copolymer was calculated by GPC (Supporting Information Figure S2B) and was found to be M_n = 7789 Da; M_w = 13933 with molecular weight distribution of 1.78. Polymers with varying ratios of 2-hydroxyethyl disulfide were characterized by ^{1}H-NMR (Supporting Information Figure S3B, S3C) and GPC (Supporting Information Figure S2C, S2D). In ^{1}H-NMR, as the molar ratio increased, the ratio of disulfide linkages in polymer backbone increased along with molecular weight of polymer. Molecular weight (M_n) of multiblock copolymers with 50% and 70% molar ratio of 2-hydroxyethyl disulfide were 9961 Da and 29873 Da respectively.

3.2 Conjugation of folic acid to the multiblock copolymer

Folic acid was conjugated to terminal hydroxyl group of the multiblock copolymer via DCC-NHS coupling. γ-Carboxylic acid of folic acid was activated by DCC-NHS and activated folic acid was then reacted with hydroxyl groups of the multiblock copolymer. In FTIR spectrum (Supporting Information Figure S4 B), intensity of N-H stretching at 3300 cm^{-1} and 1682 cm^{-1} increased after folate conjugation as compared to non-conjugated multiblock copolymer. C/N ratio of folate conjugated polymer obtained from CHN analysis was found to be 21.1. Based on calculations from C/N ratio, ~1 molecule of folic acid was found to be conjugated to the polymer. Energy dispersive X-ray spectroscopy (EDX) also showed increased nitrogen content after folate conjugation (0.55% in multiblock copolymer vs. 0.80% in folic acid conjugated multiblock copolymer) indicating successful conjugation of folic acid with the multiblock polymer.

3.3. Size and morphological characterization of polymer nanoparticles

Self-assembled polymer nanoparticles were prepared in aqueous medium by nanoprecipitation method developed by Fessi et al.[39] It was observed that folate conjugated MB-30-ss multiblock copolymer self-assembled to form stable nanoparticles based on molecular weight fraction of the PEG blocks (~20%). As the hydrophobic fraction in the multiblock copolymer increased, size of polymeric nanoparticles also increased. DLS showed folate conjugated MB 30-ss nanoparticle size in the range of ~116 nm with narrow polydispersity index while folate conjugated MB 50-ss NPs and MB 70-ss NPs showed higher particle size with high polydispersity due to more hydrophibic fraction as shown in Table 3. Folate and trastuzumab conjugated MB-30-ss NPs were also characterized by DLS SEM, AFM and TEM as shown in Figure 1, DLS shows the size range of folate and trastuzumab conjugated nanoparticles in the range of ~132.6 nm with PDI in the range of 0.175 while AFM, SEM and TEM showed particle size in the range of ~80 nm.

Table 3 Particle size from different folate conjugated polymers

Polymer notation	Size (DLS) (nm)	PDI	Zeta potential (eV)
MB-30-ss	116 ± 2.4	0.234 ± 0.010	-27.8 ± 2.30
MB-50-ss	684.8 ± 10.4	0.457 ± 0.014	-14.9.6 ± 3.60
MB-70-ss	715.1 ± 22.4	0.562 ± 0.018	-7.0 ± 2.80

(Mean ± SD, n=3)

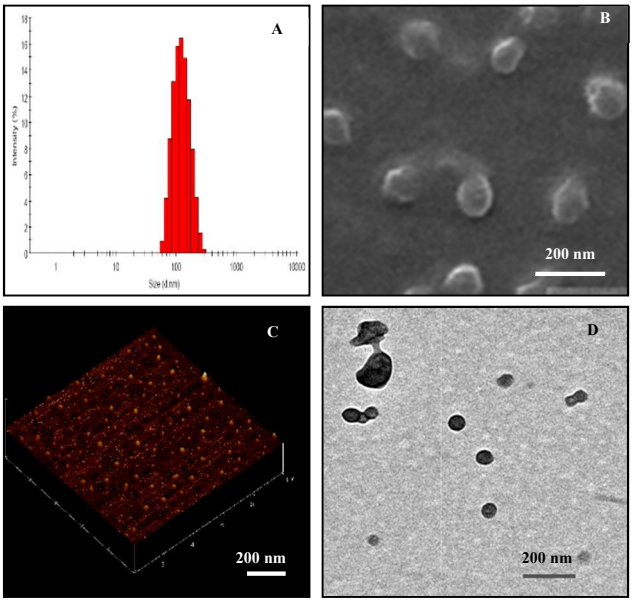

Fig. 1 Size of MB-30-ss-FA-Her-Dox-NPs (A) DLS, (B) SEM, (C) AFM and (D) TEM

3.4. Colloidal stability

Colloidal stability of polymeric nanoparticles is an essential parameter for clinical use and for drug delivery applications. Aggregation of nanoparticles can result in clogging of blood vessels leading to life threatening complications. Hence, colloidal stability of polymeric nanoparticle dispersions was studied in different media by DLS (Supporting Information Figure S5). PEGylation render stabilizing effect on NPs which was evident when nanoparticles were incubated with different dispersion media. The MB-30-ss NPs were found to be stable in 0.9% NaCl and DMEM medium. Nanoparticle stability was additionally studied in 10 mM GSH, since GSH is a naturally occurring reducing agent present in the cytosol.[26] Particle size of NPs steadily increased in presence of 10 mM GSH due to action of GSH on redox responsive disulfide linkages in the nanoparticles resulting in aggregation of polymer units causing increase in particle size.

3.5. Protein adsorption study

Opsonization and phagocytic uptake of nanoparticles is a challenge in polymeric nanoparticles for drug delivery during systemic circulation. Albumin, the most abundant protein in the blood, gets easily adsorbed on hydrophobic or charged particle surfaces. Polymeric nanoparticles based on MB-30-ss-NPs showed protein adsorption of 22 ± 1.6%. Hydrophilic PEG units provide stealth character to the NPs and thus avoids protein adsorption, rendering NPs invisible to the phagocytic/dendritic cells and macrophages of the reticulo-endothelial system (RES).[22, 42]

3.6. Blood compatibility studies

The interaction of polymer nanoparticles MB-30-ss with blood was analyzed by hemolysis studies. For intravenously administrated formulations, blood compatibility of polymeric nanocarriers is necessary. Hemolysis study of MB-30-ss-NPs was carried out by determining hemoglobin released from the RBCs after incubation with 0.5-2 mg/mL of polymer nanoparticles by UV-visible spectrophotometry. Generally, hemolysis value less than 20% is considered acceptable for polymeric nanocarriers. [43, 44]

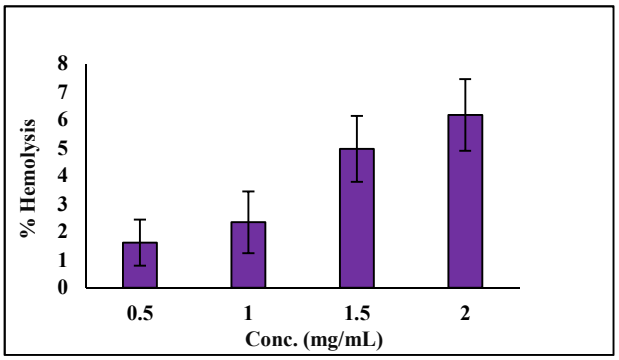

Fig.2 Hemolytic activity of polymer nanoparticles (Mean±SD, n=3)

The polymer nanoparticles exhibited low hemolytic activity for the concentrations studied (0.5-2 mg/mL). At concentration of 2 mg/mL, 6.18% hemolysis was observed while lower concentrations showed lower hemolysis as seen in Figure 2 indicating hemocompatibility of polymeric NPs.

3.7. Drug loading and release

Doxorubicin loading in the polymeric nanoparticles was enhanced using the technique developed by Sanson et al.[40] Doxorubicin was loaded in polymeric nanoparticles at pH 10.5 where doxorubicin hydrochloride is converted to hydrophobic doxorubicin free base. Also, above its pKa of 8.94, doxorubicin remains unionized which lead to efficient partitioning of doxorubicin from aqueous external medium into the hydrophobic compartment of the polymer nanoparticles. With this technique, we were able to achieve higher doxorubicin loading content of ~26%. Drug release was studied in different media including neutral and acidic pH in presence and absence of 10 mM GSH to simulate cytosolic and endocytic environments of cancer cells.

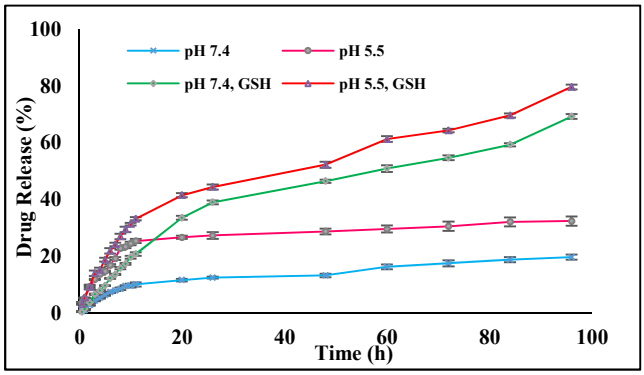

Fig. 3 Drug release profile of polymer nanoparticles at pH 5.5 and 7.4 with and without 10 mM GSH (Mean ± SD, n=3)

As shown in Figure 3, minimal drug release (~18%) was observed in pH 7.4 at 96 h while ~32% drug was released at pH 5.5 under similar conditions. In presence of 10 mM GSH, accelerated drug release of ~69% and ~80% was observed at pH 7.4 and pH 5.5 respectively at 96 h. Presence of GSH in the release medium enhanced drug release due to breaking of disulfide linkage in the polymer backbone by reversible disulfide-thiol exchange reaction between disulfide group of polymer and thiol group of GSH. Thus, due to glutathione sensitive linkages in the polymer nanoparticles, efficient drug release can be anticipated in intracellular environment in cancer cells.

3.8. Trastuzumab conjugation with polymer nanoparticles and its characterization

Trastuzumab conjugated polymeric nanoparticles were characterized by zeta potential measurement, EDX and XPS analysis. As shown in Table 4, zeta potential of the polymer nanoparticles before and after trastuzumab conjugation was determined using DLS. Trastuzumab conjugated polymeric nanoparticles showed positive shift in zeta potential of NPs due to positive charge of trastuzumab, thus suggesting conjugation of trastuzumab on the polymer nanoparticles surface.[45] Increased nitrogen content observed in EDX results also confirmed trastuzumab conjugation with nanoparticles.

XPS was further used to confirm trastuzumab conjugation on polymer nanoparticles by analyzing surface chemistry of polymer nanoparticles as shown in Figure 4. Trastuzumab conjugated polymer showed higher nitrogen peak in the binding energy region of 398-400 eV due to nitrogen of trastuzumab, indicating successful trastuzumab conjugation on nanoparticles. Trastuzumab concentration on polymersomes surface was found to be 55.4 µg/mg based on Biuret assay of unconjugated trastuzumab from the filtrate.

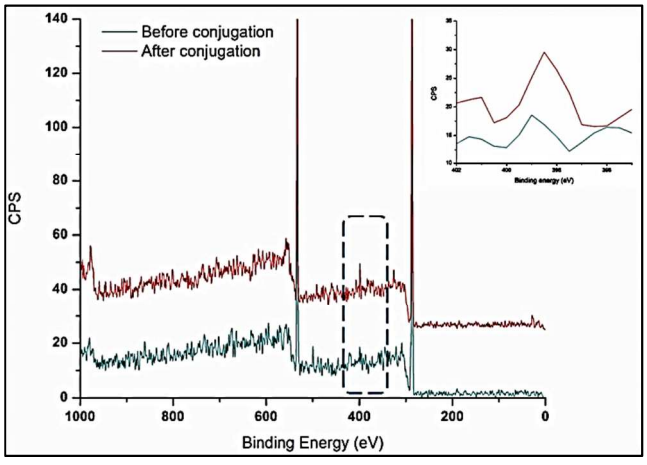

Fig. 4 XPS spectra of polymer nanoparticles before and after trastuzumab conjugation. XPS spectra show strong peak in the binding energy range 398-400 eV in trastuzumab conjugated polymer nanoparticles

Table 4 Zeta potential, size and nitrogen content of polymeric nanoparticles

Targeted polymer nanoparticles	Zeta potential(eV)	Size (nm)	Nitrogen content % (EDX)
MB-30-ss-NPs	-28.5 ± 2.2	104.2 ± 3.8	0.55

MB-30-ss-Dox-NPs	-20.2 ± 1.2	112.6 ± 2.6	8.96
MB-30-ss-FA-Dox-NPs	-16.4 ± 0.9	116.2 ± 2.4	10.24
MB-30-ss-Her-Dox-NPs	-4.4 ± 0.5	124.7 ± 3.2	12.68
MB-30-ss-FA-Her-Dox-NPs	-7.1 ± 0.9	132.6 ± 3.8	15.34

3.9. Cell viability studies

Cell viability of BT474, MCF-7 and L929 on treatment with multiblock nanoparticles was determined by MTT assay. BT474 cells overexpress HER-2 receptors,[46] while MCF-7 cells overexpress folate FRα receptors.[47] L929 is a normal cancer cell line and do not express either folate FRα or HER2 receptors.[48]

As shown in Figure 5, non-conjugated polymeric nanoparticles showed >90% viability at all concentrations from 0.25-2 mg/mL in MCF-7, BT474 and L929 cell line and thus found to be biocompatible. MTT assay was also carried out with doxorubicin loaded polymeric nanoparticles with folate and/or trastuzumab conjugation. In BT474 cell line, trastuzumab conjugated polymeric nanoparticles showed higher toxicity as compared to folate conjugated polymeric nanoparticles because of overexpressed HER2 receptors while in MCF-7 cells, folate conjugated polymeric nanoparticles showed higher toxicity because MCF-7 expresses more folate FRα receptors as compared to HER2 receptors. Dual (trastuzumab and folate) conjugated polymeric nanoparticles showed more toxicity as compared to single targeted nanoparticles in both the cell lines. L929 does not express FRα and HER2 receptors and hence exhibits less toxicity as compared to BT474 and MCF-7 cell line.

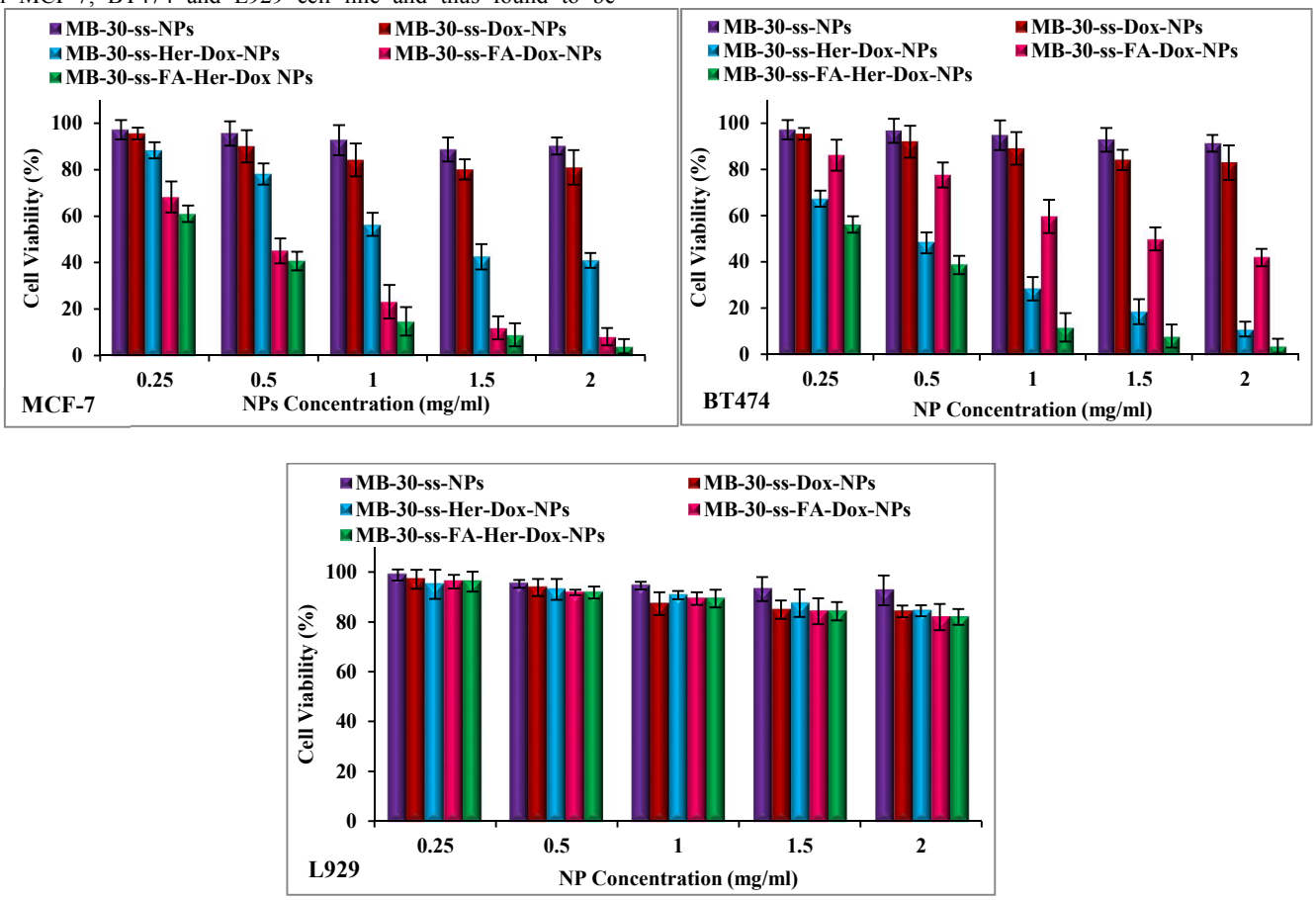

Fig. 5 Cell viability of polymeric nanoparticles in MCF-7, BT474, L929 by MTT assay (Mean ± SD, n=3)

3.9.1. Cellular uptake studies by confocal laser scanning microscopy

Cellular uptake of polymer nanoparticles was examined to evaluate targeting efficiency of NPs in BT474, MCF-7 and in L929 cancer cell lines. As shown in Figure 6, in case of BT474 and MCF-7 cancer cells, MB-30-ss-FA-Dox-NPs and MB-30-ss-Her-Dox-NPs showed higher cellular uptake as compared to non-targeted nanoparticles through folate FRα and HER2 receptor mediated endocytosis respectively resulting in higher accumulation of NPs in the cells. Dual targeted MB-30-ss-FA-Her-Dox-NPs showed higher doxorubicin fluorescence intensity as compared to MB-30-ss-FA-Dox-NPs and MB-30-ss-Her-Dox-NPs, indicating higher cellular uptake of MB-30-ss-FA-Her-Dox-NPs as compared to cells treated with single targeted nanoparticles. This can be ascribed to dual folate FRα and HER2 receptor mediated endocytosis of the MB-30-ss-FA-Her-Dox-NPs.

L929 cell line which does not overexpress FRα or HER2 receptors showed low fluorescence intensity with MB-30-ss-FA-Dox-NPs, MB-30-ss-Her-Dox-NPs and MB-30-ss-FA-Her-Dox-NPs. The fluorescence intensity was low and similar in all four types of polymeric nanoparticles showing non-specific cellular uptake of polymeric nanoparticles.

3.9.2. Cellular uptake studies by using flow cytometry

Cellular uptake of nanoparticles was studied in BT474, MCF-7, and L929 cell lines using flow cytometry to further evaluate cellular uptake efficiency of polymer nanoparticles. As shown in Figure 7, in case of MCF-7 and BT474 cells, MB-30-ss-FA-Dox-NPs and MB-30-ss-Her-Dox-NPs showed ~9 fold increase in fluorescence intensity as compared to MB-30-ss-Dox-NPs. This increment in fluorescence intensity is due to the folate/trastuzumab mediated endocytosis. MB-30-ss-FA-Her-Dox-NPs showed ~20 fold increase in fluorescence intensity as compared to MB-30-ss-Dox-NPs, indicating their higher targeting efficiency. In L929 cells, low fluorescence intensity were observed with all four type of polymeric nanoparticles. Thus, FACS cellular uptake studies agree with the confocal studies regarding superior uptake of dual targeted polymer nanoparticles in cancer cells.

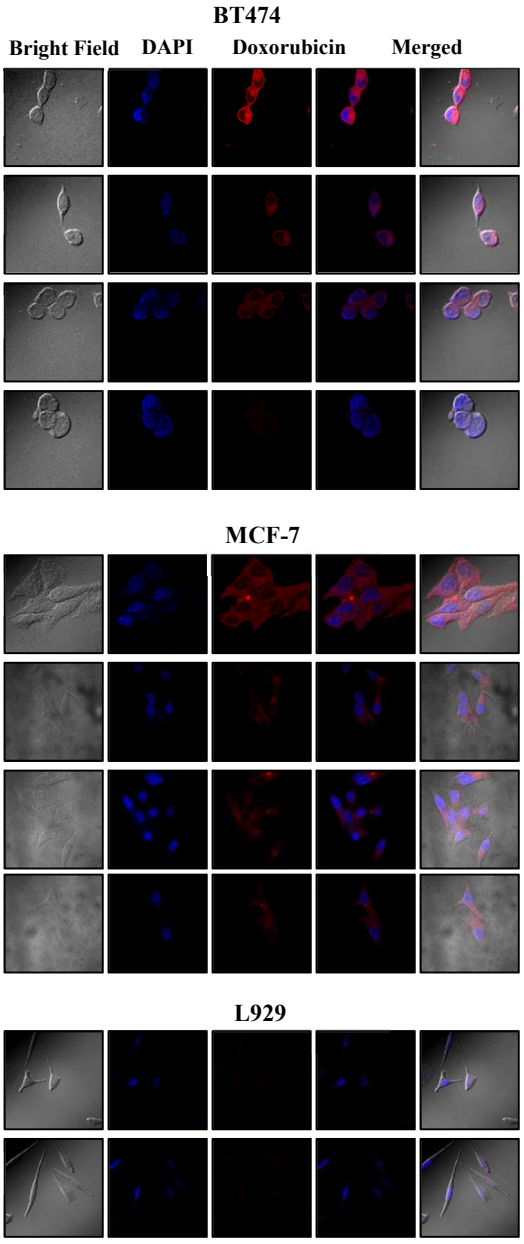

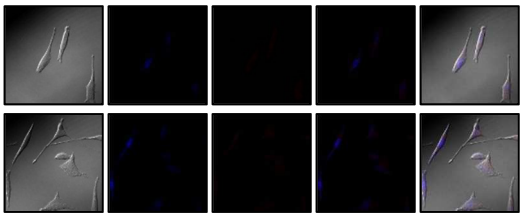

Fig. 6 Cellular uptake of polymer nanoparticles in BT474, MCF-7 and L929 cells (A) MB-30-ss-FA-Her-Dox-NPs (B) MB-30-ss-Her-Dox-NPs (C) MB-30-ss-FA-Dox-NPs (D) MB-30-ss-Dox-NPs

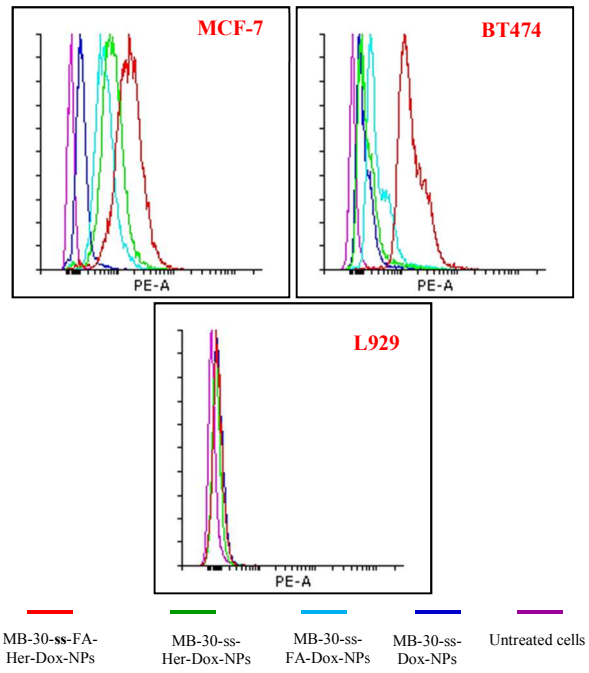

Fig. 7 Cellular uptake of polymeric nanoparticles in cell lines, BT474, MCF-7 and L929 by flow cytometry

3.9.3. Apoptosis assay

After nanoparticle treatment with cells, apoptotic/necrotic cells were distinguished from healthy cells by Annexin V-FITC assay. Annexin V, a phospholipid binding protein, binds selectively to exposed phosphatidylserine and detects apoptotic cells. Apoptotic cells can be differentiated from viable and necrotic cells based on selective uptake of Annexin V and propidium iodide.[49]

As shown in Figure 8, in case of MCF-7 and BT474 cells, single targeted polymer nanoparticles (MB-30-ss-FA-Dox-NPs and MB-30-ss-Her-Dox-NPs) showed higher apoptotic and necrotic cells as compared to MB-30-ss-Dox-NPs which can be ascribed to FRα and HER2 receptor mediated endocytosis. Dual targeted polymer nanoparticles (MB-30-ss-FA-Her-Dox-NPs) showed higher apoptotic and necrotic cells as compared to single targeted and non-targeted polymer nanoparticles in BT474 and MCF-7 showing higher targeting efficiency resulting in higher apoptosis in cancer cells. In case of L929 cells, majority of the cells were healthy due to minimal cellular uptake of nanoparticles irrespective of attached ligands indicating their non-toxicity to the normal cell line.

3.10. Animal studies

Ehrlich ascites tumor (EAT) is characterized by high transplantable capability and rapid proliferation rate. The EAT cells were cultured in mice by transplanting liquid ascites form in the peritoneal cavity of mouse. EAT cells express folate FRα and HER2 receptors and hence was selected for our experiments.[50]

Therapeutic efficacy of MB-30-ss-FA-Her-Dox-NPs was investigated for their antitumor activity in the mice bearing Ehrlich ascites tumor. When the volume of tumor increased up to 200-250 mm^3 in the mice, mice were administered with MB-30-ss-FA-Her-Dox-NPs, free doxorubicin and saline (control).

As shown in Figure 9, progressive increment in tumor size (up to 986% on 18th day) was observed in the control group. The mice treated with doxorubicin showed moderate antitumor activity with ~42% decrease in tumor size, whereas MB-30-ss-FA-Her-Dox-NPs showed significant antitumor effect as compared to the control and free doxorubicin treated mice with ~88% decrease in tumor size.

The improved antitumor activity of MB-30-ss-FA-Her-Dox-NPs can be attributed to longer blood circulation of polymeric nanoparticles due to PEG chains, dual targeting approach and GSH triggered increased intracellular doxorubicin release due to multiple disulfide linkages in polymer nanoparticles.

Relative body weight changes of the treated Swiss albino mice were observed and analyzed for determining systemic adverse effects of the free drug and NPs treatment. As shown in Supporting Information Figure S8, free doxorubicin treated mice showed significant weight loss over the period of treatment indicating systemic toxicity of free drug. At day 18, about ~12 % decrease in body weight was observed with free doxorubicin treated mice whereas polymeric NPs formulation (MB-30-ss-FA-Her-Dox-NPs) showed only slight reduction in weights of mice ~5% indicating their relative non-toxicity due to active targeting and redox responsive linkages in polymeric nanoparticles leading to higher bioavailability of doxorubicin at tumor site. The observed systemic adverse effects of the free doxorubicin and relative non-toxicity of the nanoparticle formulation were further evaluated using histopathology studies of vital organs and serum biochemistry studies of the treated Swiss albino mice.

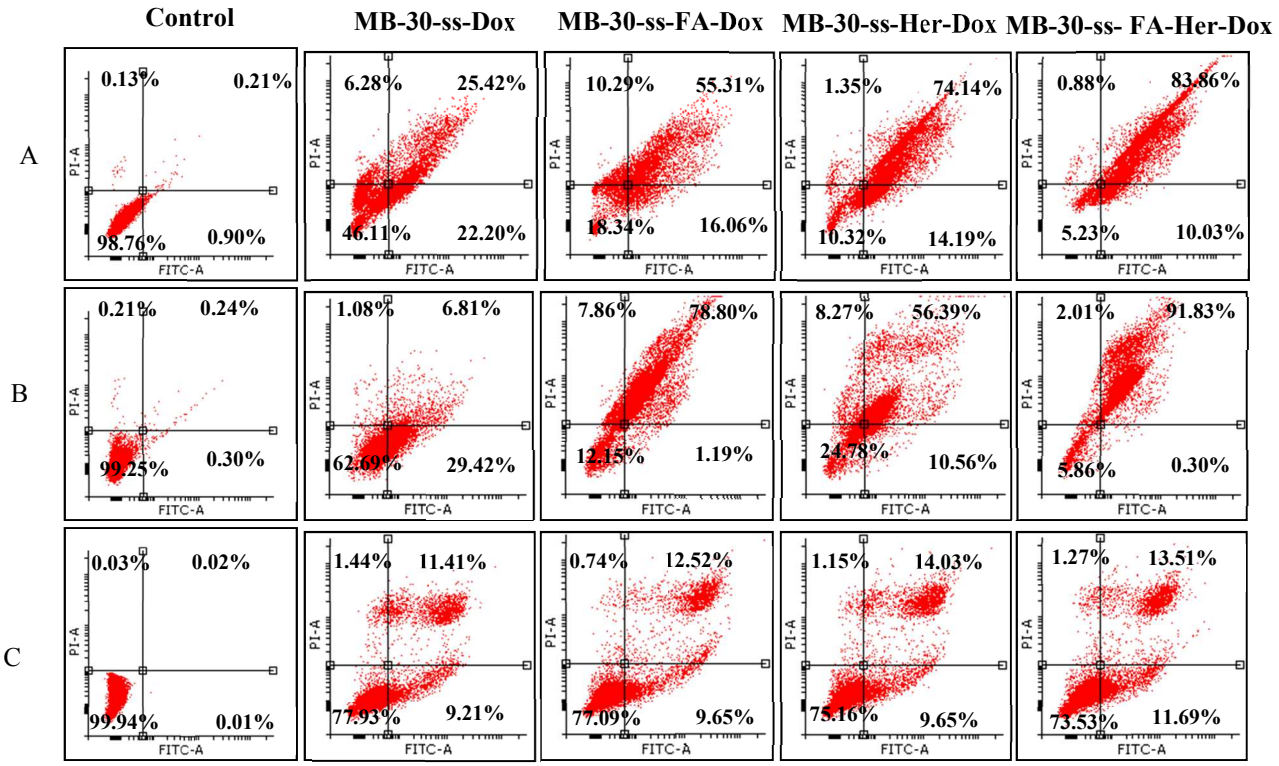

Fig. 8 Annexin V-FITC apoptosis assay in (A) BT474, (B) MCF-7 and (C) L929 cell lines by using flow cytometry

Cite this: DOI: 10.1039/c0xx00000x

www.rsc.org/xxxxxx

PAPER

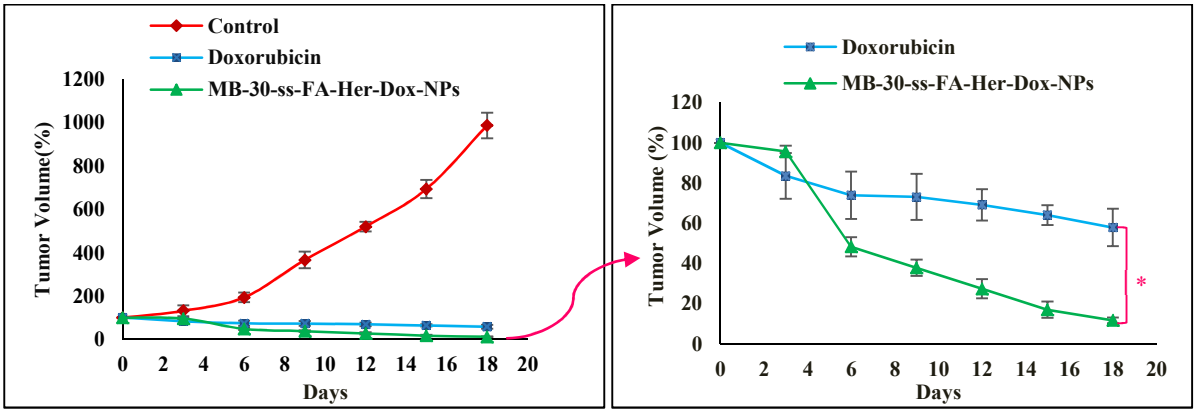

Fig. 9 *In vivo* efficacy of folic acid and trastuzumab conjugated doxorubicin loaded polymer nanoparticles, doxorubicin and PBS treated mice (control). Data are shown as mean ± S.D, n=6. *p-value < 0.05.

3.11. Toxicological studies

3.11.1. Histopathology

Antitumor efficacy of MB-30-ss-FA-Her-Dox-NPs was also determined using histopathological analysis of tumor. Tumor sections of control mice exhibited viable tumor cells with active proliferation while doxorubicin treated mice showed necrosis area at center and viable tumor in the periphery as shown in Figure 10. MB-30-ss-FA-Her-Dox-NPs showed whole tumor necrosis with absence of residual tumor cells and proliferating fibroblasts indicating enhanced antitumor efficacy of MB-30-ss-FA-Her-Dox-NPs.

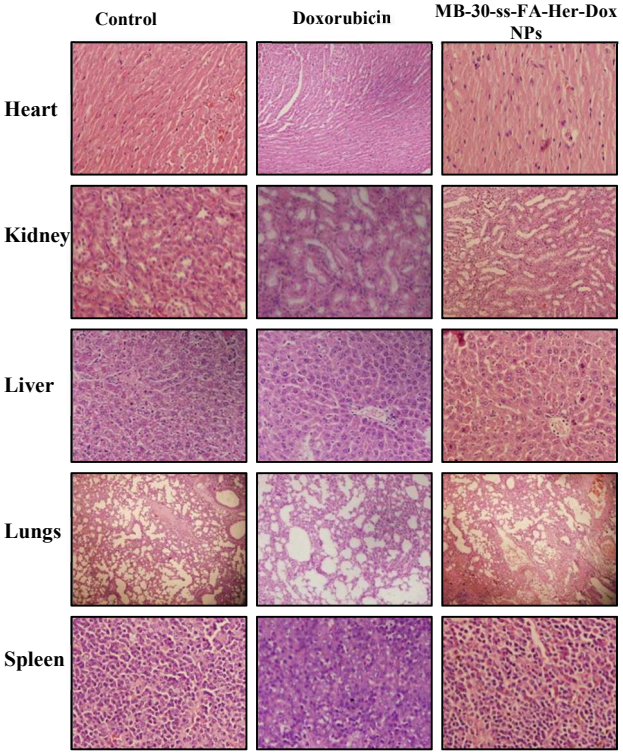

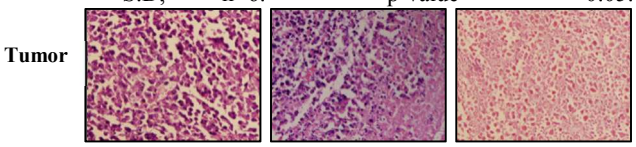

Fig. 10 Histopathological images of sections of heart, kidney, liver, lungs, spleen and tumor

Histopathology of vital organs like heart, liver, lungs, kidney and spleen were analyzed for any toxic effects of nano-formulations on these vital organs. As shown in Figure 10, heart section of mice treated with free doxorubicin showed cardiomyocyte swelling with significant cytoplasmic vacuolization indicating cardiotoxicity of doxorubicin. MB-30-ss-FA-Her-Dox-NPs formulation showed mild cardiomyocyte swelling with minimal cytoplasmic vacuolization indicating their cardiac biocompatibility.

Liver sections of mice treated with doxorubicin showed hepatotoxity with spotty necrosis and kupffer cell prominence. Substantial tubular damage was also detected in kidney with doxorubicin treated mice. MB-30-ss-FA-Her-Dox-NPs exhibited comparable histology as that of control indicating non-toxicity to these vital organs.

Glutathione sensitivity and dual targeting ability of MB-30-ss-FA-Her-Dox-NPs can be responsible for their observed non-toxicity since they allowed cancer specific targeting of polymeric nanoparticles resulting in higher accumulation in tumor.

3.11.2. Serum biochemistry

To investigate effect of MB-30-ss-FA-Her-Dox-NPs on vital organs, serum was analyzed for biochemical parameters as shown in Table 5.

Table 5 Serum biochemistry analysis

Parameter	Control (PBS)	Doxorubicin	MB-30-ss-FA-Her-Dox-NPs
Total Bilirubin (mg/dL)	0.24 ± 0.04	0.54 ± 0.04	0.38 ± 0.01
SGOT(AST) (IU/L)	65.14 ± 1.60	128.26 ± 3.40	72.40 ± 1.88
SGPT(ALT) (IU/L)	38.42 ± 1.86	80.48 ± 2.60	45.80 ± 1.64
Alkaline phosphatase (IU/L)	142.12 ± 2.10	232.60 ± 5.80	148.12 ± 2.82
Total Protein (g/dL)	6.92 ± 0.12	6.68 ± 0.18	7.62 ± 0.20
Albumin (g/dL)	4.54 ± 0.28	3.64 ± 0.14	3.66 ± 0.16
Globulin (g/dL)	2.32 ± 0.18	1.76 ± 0.06	1.90 ± 0.01
A:G Ratio	2.28 ± 0.20	2.42 ± 0.02	2.38 ± 0.12
Total Cholesterol (mg/dL)	128.94 ± 2.92	142.80 ± 1.74	136.12 ± 2.34
Blood urea (mg/dL)	41.48 ± 2.40	80.76 ± 1.58	46.68 ± 1.22
Creatinine (mg/dL)	0.36 ± 0.02	0.74 ± 0.04	0.44 ± 0.02
Uric acid (mg/dL)	2.98 ± 0.18	7.62 ± 0.22	2.68 ± 0.24
Calcium (mg/dL)	8.80 ± 0.26	8.34 ± 0.24	8.68 ± 0.20
Phosphorus (mg/dL)	3.12 ± 0.16	4.10 ± 1.12	3.00 ± 0.26
CK-MB (IU/L)	1.98 ± 0.56	11.34 ± 1.80	4.18 ± 0.60

All value are expressed as mean ± SD (n=3). Highlighted values show p-value < 0.05.

Creatinine kinase MB (CK MB) is often detected in serum after cardiac injury and hence it was analyzed in serum to detect cardiotoxicity in mice.[51] The level of CK MB in serum was found to be higher in doxorubicin treated mice ($p < 0.05$) as compared to control indicating cardiotoxicity. MB-30-ss-FA-Her-Dox-NPs treated mice showed statistically insignificant difference in CK MB values as compared to control ($p > 0.05$) showing non-toxicity to cardiac tissues.

Liver specific enzymes namely alanine transaminases (ALT), aspartate transaminases (AST) and alkaline phosphatase (ALP) were determined to evaluate liver toxicity of nanoformulations. Significant increase in ALT, AST and ALP levels were observed in doxorubicin treated mice as compared to control ($p < 0.05$), whereas MB-30-ss-FA-Her-Dox-NPs treated mice indicated statistically insignificant increase in their values indicating non-toxicity to the liver. Renal parameters like urea, creatinine and uric acid levels were also higher in case of doxorubicin treated mice as compared to control showing nephrotoxicity, whereas MB-30-ss-FA-Her-Dox-NPs showed similar levels of these biomarkers as that of control indicating non-toxicity to kidney.

4. Conclusions

In conclusion, glutathione sensitive folate conjugated random multiblock copolymer was successfully synthesized and formed self-assembled nanoparticles which were further conjugated to trastuzumab with final particle size of ~80 nm. Biocompatible studies based on hemolysis, coagulation and MTT assay demonstrated their suitability for *in vivo* use. Dual targeted multiblock copolymer nanoparticles showed enhanced cellular uptake and apoptosis in breast cancer cell lines as compared to single targeted and non-targeted multiblock copolymer nanoparticles. *In vivo* studies of Dual targeted multiblock copolymer nanoparticles showed significant reduction in tumor volume as compared to free doxorubicin without significant toxicity to heart, liver or kidney, demonstrating potential of these nanocarriers for drug delivery in cancer therapy.

Acknowledgments

Authors are thankful to the Department of Biotechnology (DBT), India, for the research grant (BT/PR13341/NNT/28/467/2009). Arun Kumar is thankful to Council of Scientific and Industrial Research, India for providing senior research fellowship. He is thankful to Dr. Archna Bansal and Prof. Renu Saxena from All India Institute of Medical Science (AIIMS), New Delhi, for their help in CK-MB determination. The Author is also thankful to Dr. Alok C. Bharti and Dr. Shyam B. Prasad from ICPO Noida, for their help in flow cytometry. He is also thankful to Dr. Nadeem Tanveer, University College of Medical Sciences, Delhi for his help with histopathological analysis.

Notes and references

[a] *Centre for Biomedical Engineering, Indian Institute of Technology Delhi, New Delhi 110016, India Tel: +91 1126591041*
E-mail: veenak_iitd@yahoo.com
[b] *Biomedical Engineering Unit, All India Institute of Medical Sciences (AIIMS), New Delhi 110029, India Tel: +91 1126591041*
[c] *Department of Pathology, All India Institute of Medical Sciences (AIIMS), New Delhi 110029, India*
[d] *Centre for Polymer Science and Engineering, Indian Institute of Technology Delhi, New Delhi 110016, India*

† Electronic Supplementary Information (ESI) available: [^{1}H NMR spectra of triblock copolymers and multiblock copolymers, GPC data of triblock copolymer and multiblock copolymers, FTIR spectra of multiblock copolymer and folic acid conjugated multiblock copolymer, colloidal stability of polymer nanoparticles, Comparison of molecular weights of PEG, triblock copolymer and multiblock copolymers and relative body weight of swiss albino mice during the treatment]. See DOI: 10.1039/b000000x

1 S. Lv, M. Li, Z. Tang, W. Song, H. Sun, H. Liu and X. Chen, *Acta Biomater.*, 2013, **9,** 9330-9342.
2. C. Y. Ang, S. Y. Tan and Y. Zhao, *Org. Biomol. Chem.*, 2014, **12,** 4776-4806.
3. K. Letchford and H. Burt, *Eur. J. Pharm. Biopharm.*, 2007, **65,** 259-269.
4. T. Krasia-Christoforou and T. K. Georgiou, *J. Mater. Chem. B*, 2013, **1,** 3002-3025.
5. V. Delplace, P. Couvreur and J. Nicolas, Polym. Chem., 2014, 5, 1529-1544.
6. A. Wicki, D. Witzigmann, V. Balasubramanian and J. Huwyler, *J. Controlled Release*, 2015, **200,** 138-157.
7. A. Rosler, G. W. Vandermeulen and H. A. Klok, *Adv. Drug delivery Rev.*, 2012, **64,** 270-279.
8. E. Perez-Herrero and A. Fernandez-Medarde, *Eur. J. Pharm. Biopharm.*, 2015, **93,** 52-79.
9. M. Huo, J. Yuan, L. Tao and Y. Wei, Polym. Chem., 2014, 5, 1519-1528.
10. D. Peer, J. M. Karp, S. Hong, O. C. Farokhzad, R. Margalit and R. Langer, *Nat. Nanotechnol.*, 2007, **2,** 751-760.
11. N. R. Ko and J. K. Oh, *Biomacromolecules*, 2014, **15,** 3180-3189.
12. Y. Zhang, J. He, D. Cao, M. Zhang and P. Ni, Polym. Chem., 2014, 5, 5124-5138.
13. S. Kaur, C. Prasad, B. Balakrishnan and R. Banerjee, *Biomaterials Science*, 2015, DOI: 10.1039/C5BM00002E.
14. C. Cui, P. Yu, M. Wu, Y. Zhang, L. Liu, B. Wu, C. X. Wang, R. X. Zhuo and S. W. Huang, *Colloids Surf., B,* 2015, **129,** 137-145.

15. A. Kumar, S. V. Lale, S. Mahajan, V. Choudhary and V. Koul, *ACS Appl. Mater. Interfaces*, 2015, **7,** 9211-9227.
16. B. Wu, P. Yu, C. Cui, M. Wu, Y. Zhang, L. Liu, C. X. Wang, R. X. Zhuo and S. W. Huang, *Biomaterials Science*, 2015, **3,** 655-664.
17. C. Shi, X. Guo, Q. Qu, Z. Tang, Y. Wang and S. Zhou, *Biomaterials*, 2014, **35,** 8711-8722.
18. D. J. Phillips, J. P. Patterson, R. K. O'Reilly and M. I. Gibson, Polym. Chem., 2014, 5, 126-131.
19. Y. Zhong, W. Yang, H. Sun, R. Cheng, F. Meng, C. Deng and Z. Zhong, *Biomacromolecules*, 2013, **14,** 3723-3730.
20. S. V. Lale, A. Kumar, S. Prasad, A. C. Bharti and V. Koul, *Biomacromolecules*, 2015, **16,** 1736-1752.
21. Y. Zhong, F. Meng, C. Deng and Z. Zhong, *Biomacromolecules*, 2014, **15,** 1955-1969.
22. S. V. Lale, R. G. Aswathy, A. Aravind, D. S. Kumar and V. Koul, *Biomacromolecules*, 2014, **15,** 1737-1752.
23. N. Bertrand, J. Wu, X. Xu, N. Kamaly and O. C. Farokhzad, *Adv. Drug Delivery Rev.*, 2014, **66,** 2-25.
24. H. K. Patra and A. P. Turner, *Trends Biotechnol.*, 2014, **32,** 21-31.
25. B. Hoang, R. M. Reilly and C. Allen, *Biomacromolecules*, 2012, **13,** 455-465.
26. M. C. Figueroa-Magalhaes, D. Jelovac, R. M. Connolly and A. C. Wolff, *Breast*, 2014, **23,** 128-136.
27. R. F. Storey and J. W. Sherman, *Macromolecules*, 2002, **35,** 1504-1512.
28. C. M. Dong, K. Y. Qiu, Z. W. Gu and X. D. Feng, *Macromolecules*, 2001, **34,** 4691-4696.
29. S. J. Bae, M. K. Joo, Y. Jeong, S. W. Kim, W. K. Lee, Y. S. Sohn and B. Jeong, *Macromolecules*, 2006, **39,** 4873-4879.
30. O. Jeon, S. H. Lee, S. H. Kim, Y. M. Lee and Y. H. Kim, *Macromolecules*, 2003, **36,** 5585-5592.
31. D. Cohn, T. Stern, M. F. Gonzalez and J. Epstein, *J. Biomed. Mater. Res.*, 2002, **59,** 273-281.
32. C. T. Huynh, M. K. Nguyen, J. H. Kim, S. W. Kang, B. S. Kim and D. S. Lee, *Soft matter*, 2011, **7,** 4974-4982.
33. M. Pechar, K. Ulbrich, V. Šubr, L. W. Seymour and E. H. Schacht, *Bioconjugate Chem.*, 2000, **11,** 131-139.
34. M. Ding, Z. Qian, J. Wang, J. Li, H. Tan, Q. Gu and Q. Fu, *Polym. Chem.*, 2011, **2,** 885-891.
35. K. Na, K. H. Lee, D. H. Lee and Y. H. Bae, *Eur. J. Pharm. Sci.*, 2006, **27,** 115-122.
36. S. Yu, C. He, J. Ding, Y. Cheng, W. Song, X. Zhuang and X. Chen, *Soft Matter*, 2013, **9,** 2637-2645.
37. S. Yu, J. Ding, C. He, Y. Cao, W. Xu and X. Chen, *Adv. Healthc. Mater.*, 2014, **3,** 752-760.
38. X. Li, Y. Wang, J. Chen, Y. Wang, J. Ma and G. Wu, *ACS Appl. Mater. Interfaces*, 2014, **6,** 3640-3647.
39. H. Fessi, F. Puisieux, J. P. Devissaguet, N. Ammoury and S. Benita, *Int. J. Pharm.*, 1989, **55,** R1-R4.
40. C. Sanson, C. Schatz, J. F. Le Meins, A. Soum, J. Thévenot, E. Garanger and S. Lecommandoux, *J.Controlled Release*, 2010, **147,** 428-435.
41. T. Mosmann, *J.Immunol. Methods*, 1983, **65,** 55-63.
42. R. Gref, M. Luck, P. Quellec, M. Marchand, E. Dellacherie, S. Harnisch, T. Blunk and R. H. Muller, *Colloids Surf. B*, 2000, **18,** 301-313.
43. K. Amin and R. M. Dannenfelser, *J. Pharm. Sci*, 2006, **95,** 1173-1176.
44. J. F. Krzyzaniak, F. A. A. Nuúnñez, D. M. Raymond and S. H. Yalkowsky, *J. Pharm. Sci.*, 1997, **86,** 1215-1217.
45. S. V. Lale, A. Kumar, F. Naz, A. C. Bharti and V. Koul, *Polym. Chem.*, 2015, **6,** 2115-2132.
46. K. Subik, J. F. Lee, L. Baxter, T. Strzepek, D. Costello, P. Crowley, L. Xing, M. C. Hung, T. Bonfiglio and D. G. Hicks, *Breast Cancer*, 2010, **4,** 35.
47. R. Nahire, M. K. Haldar, S. Paul, A. Mergoum, A. H. Ambre, K. S. Katti, K. N. Gange, D. K. Srivastava, K. Sarkar and S. Mallik, *Biomacromolecules*, 2013, **14,** 841-853.
48. D. Bhattacharya, M. Das, D. Mishra, I. Banerjee, S. K. Sahu, T. K. Maiti and P. Pramanik, *Nanoscale*, 2011, **3,** 1653-1662.
49. R. Hingorani, J. Deng, J. Elia, C. McIntyre and D. Mittar, https://www.bdbiosciences.com/documents/BD_FACSVerse_Apoptosis_Detection_AppNote.pdf assessed on June 2015.
50. M. Ozaslan, I. D. Karagoz, I. H. Kilic and M. E. Guldur, *Afr. J. Biotechnol.*, 2013, **10,** 2375-2378.
51. D. J. Robinson and R. H. Christenson, *J. Emerg. Med.*, 1999, **17,** 95-104.

Table of Content

Dual Targeted Redox responsive doxorubicin loaded polymeric nanoparticles were prepared and evaluated for anticancer efficacy. *In vitro* studies in cancer cell lines and *in vivo* studies in Ehrlich ascites tumor bearing Swiss albino mice were carried out.

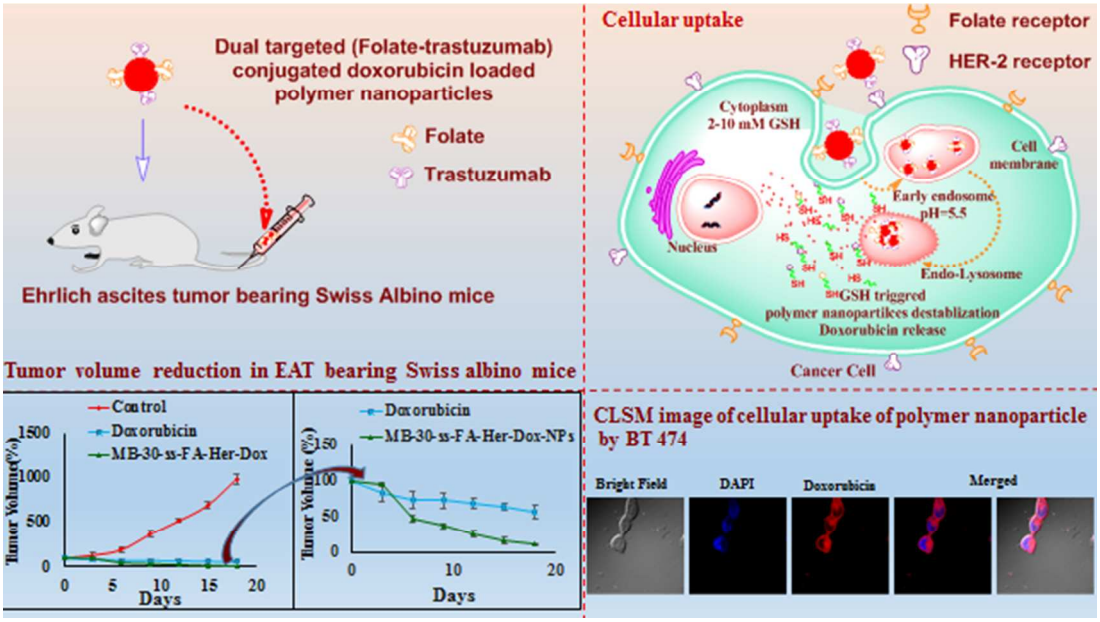

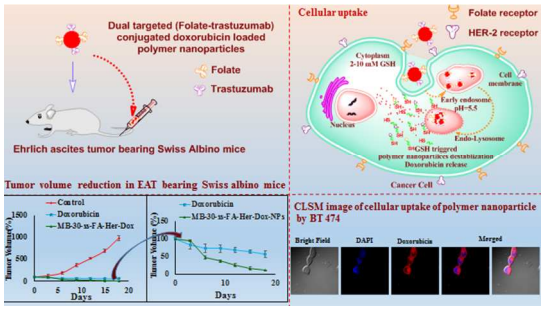

8×4 cm